Product Yields and Kinetics from the Vapor Phase Cracking of Wood Pyrolysis Tars

The homogeneous vapor phase cracking of newly formed wood pyrolysis tar was studied at low molar concentrations as a function of temperature (773-1,073 K), at residence times of 0.9-2.2 s. Tar conversions ranged from about 5 to 88%. The tars were generated by low heating rate (0.2 K/s) pyrolysis of ~2 cm deep beds of sweet gum hardwood, and then rapidly conveyed to an adjacent reactor for controlled thermal treatment. Quantitative yields and kinetics were obtained for tar cracking and resulting products formation. The major tar conversion product was carbon monoxide, which accounted for over two-thirds of the tar lost at high severities. Corresponding ethylene and methane yields were each about 10% of the converted tar. Coke formation was negligible and weight-average tar molecular weight declined with increasing tar conversion. A first-order distributed activation energy model more closely correlated tar conversion kinetics over a wider range of reaction conditions than did a single-reaction model.

Michael L. Boroson
Jack B. Howard
John P. Longwell
William A. Peters
Department of Chemical Engineering
and Energy Laboratory
Massachusetts Institute of Technology
Cambridge, MA 02139

Introduction

Wood pyrolysis, or devolatilization, in general involves a complex set of chemical reactions, often influenced by physical transport processes. Identification and modeling of the important chemical and physical rate processes for different conditions of practical and scientific interest will advance existing capabilities for simulating whole wood pyrolysis. Theoretical and experimental contributions to this end have appeared in recent years (Chan and Krieger, 1983; Kelbon et al., 1987). The present paper focuses on quantitating one feature of wood pyrolysis: the vapor phase reactions of tars just released by devolatilization of the parent material.

When wood is heated, the solid decomposes by thermal scission of chemical bonds. The species formed by this initial step may not be volatile and may undergo additional bond-breaking reactions to form volatiles or may experience condensation/polymerization reactions to form higher molecular weight products, including char. The volatile species may undergo further reaction within the particle either homogeneously in the gas phase or heterogeneously by reaction with the solid biomass or char. These intraparticle secondary reactions can be influenced by the rates of volatiles mass transfer within and away from the particle. After escaping the particle, the tars and other volatiles may still undergo secondary reactions homogeneously in the vapor phase or heterogeneously on the surface of other biomass or char particles. Depending on reaction conditions, intra- and/or extraparticle secondary reactions may exert modest to virtually controlling influence on product yields and distributions from wood pyrolysis.

There exists a significant amount of literature on the primary pyrolysis of wood; however, there appear to have been few quantitative studies on homogeneous, vapor phase secondary reaction kinetics of wood pyrolysis tars (Mattocks, 1981; Diebold, 1985; Liden, 1985). Kinetic information on the conversion kinetics of volatiles derived from two important wood constituents, cellulose and lignin (Antal, 1983), is also of interest.

The broad goal of the present study was to obtain further quantitative understanding of the secondary cracking behavior of a fresh—that is, newly generated and never stored—wood pyrolysis tar, under conditions pertinent to extraparticle homogeneous vapor phase secondary reactions. Specific objectives were:

1. To identify and quantify the major primary and secondary products of wood pyrolysis
2. To characterize primary and secondary tars in order to better understand the chemical process of tar cracking

Correspondence concerning this paper should be addressed to W. A. Peters.
The present address of M. L. Boroson is Rogers Corp., Lurie R&D Center, Rogers, CT 06263.

3. To model vapor phase tar cracking and use the data to obtain global kinetic parameters for tar cracking and for the resulting generation of individual gaseous products

These goals called for an experimental technique providing good material balances while allowing:

- Controlled generation of pyrolysis tars
- Quantification of the yields of these tars and of associated other primary volatiles (and char)
- Virtually immediate introduction of those tars to an independently controlled thermal treatment reactor
- Measurement of tar conversion and secondary products formation from reactions therein at known temperatures and residence times

Molecular weight distributions of primary and partially converted tars were also of interest.

An apparatus and operating procedures developed by Serio (1984; Serio et al., 1987) for similar studies on coal pyrolysis tars were adapted for the present needs. Two independently heated, series-connected tubular chambers served as separate tar generation and tar vapor cracking reactors. The cumulative initial tar yield (the cumulative feed to the cracking reactor), and the cumulative tar conversion from secondary reactions (the cumulative tar effluent from the cracking reactor) were respectively measured in separate experiments under duplicate tar generation conditions, without and with the cracking reactor in place. Char and other primary products, and products of secondary reactions, were measured in like manner. A broad range of tar conversions (<5 to >88%) was achieved by selecting different combinations of known temperatures and residence times in the second reactor.

Methodology

Reactor design and operation

Yields of individual primary and secondary pyrolysis products as affected by reaction conditions, and physical and chemical characteristics of primary (newly formed) and secondary (surviving thermal treatment) tar samples, were needed to fulfill the study objectives.

A two-chamber tubular reactor, Figure 1, developed by Serio (1984; Serio et al., 1987) for systematic studies of extraparticle secondary reactions of newly formed coal pyrolysis tars, was adapted for the present measurements. In this apparatus primary tar, that is, tar that has undergone minimum extraparticle secondary reactions, is generated in an upstream reactor (*Furnace-1* in Figure 1) by heating a shallow packed bed of wood, usually at a constant heating rate. Reactor 1 (Serio, 1984) consisted of a type 316 stainless steel inner tube (1.27 cm OD × 24.13 cm length × 0.089 cm wall thickness) mounted coannularly within an Incoloy 800H outer tube (2.13 cm OD × 41.91 cm length × 0.373 cm wall). Typical reactor 1 operating conditions were:

Heating rate: 0.2 K/s
Initial temperature: room temperature up to 303 K
Final temperature: 723 K
Holding time upon attaining final temperature: 1,800 s

A screen near the exit of the inner tube supported the tar source—an approximately 2 cm deep bed of 45–250 μm particles of sweet gum hardwood, an elemental analysis for which is given by Nunn (1981; Nunn et al., 1985). Sweet gum hardwood is a suitable source of tar because this type of wood has attracted

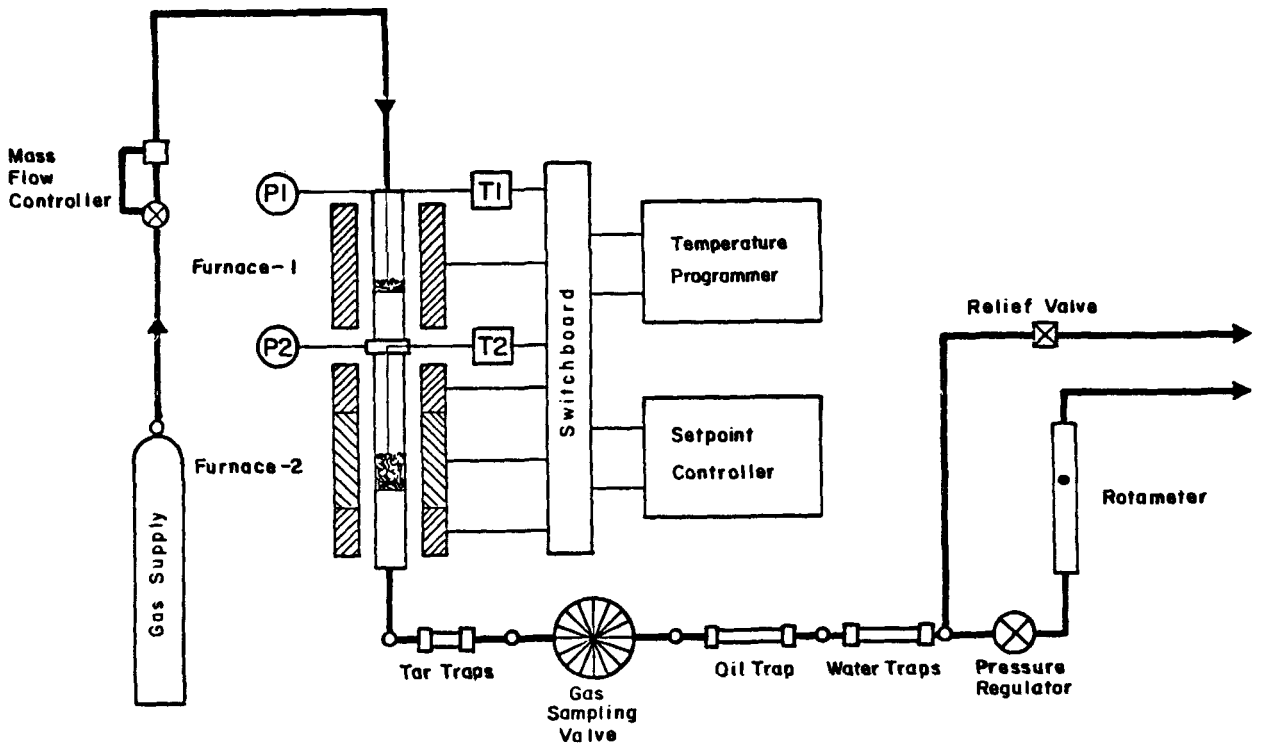

Figure 1. Two-stage reactor system.

Reprinted with permission from M. A. Serio, W. A. Peters, and J. B. Howard, "Kinetics of Vapor-Phase Secondary Reactions of Prompt Coal Pyrolysis Tars," *Ind. and Eng. Chemist. Res.*, **26**(9), 1831 (1987). Copyright (1987) American Chemical Society.

interest as an energy crop in the southern United States, and because kinetic data on the rapid devolatilization behavior (1,000 K/s) of thin samples of this hardwood are available (Nunn, 1981; Nunn et al., 1985) for comparison with the present findings.

Newly formed tar and other volatiles are rapidly swept from reactor 1 into a second reactor (*Furnace-2,* Figure 1) by a continuous flow of carrier gas (helium with an argon tracer). Using measurements of the molecular weight distribution of this newly formed tar (see below and Figure 9), the concentration of whole tar at the reactor 2 entrance was estimated at <0.4 mol %. Reactor 2 is similar in design and construction materials to reactor 1, except that the inner and outer tubes are longer—38.10 cm and 57.79 cm, respectively—and in vapor phase cracking runs there was no support for a packed bed of wood.

In reactor 2, tar and other volatiles are subjected to controlled extents of postpyrolysis thermal treatment at temperatures between 773 and 1,073 K, pressures from 120 to 250 kPa, and residence times between 0.9 and 2.2 s. Upon exiting reactor 2 (or reactor 1 in primary pyrolysis studies) products and unreacted volatiles pass through a tar trap consisting of a tube packed with Teflon wool and maintained at room temperature. Next, volatile products pass through a 15-loop gas sampling valve. Samples are collected at known times throughout the run for later gas chromatographic analysis. After the gas sample loop, the products pass successively through two collectors at room temperature: an oil trap packed with activated carbon, to collect highly volatile tars, and a water trap packed with silica gel.

Two reactor configurations have been employed in the present investigation. In mode 1 runs, only the first-stage reactor is used, and freshly evolved wood pyrolysis products spend little time at high reaction severities. The holdup (V/F) of tar between the exit of the generation bed and the entrance of reactor 2, is estimated to be <1 s. Calculations with the kinetic parameters derived in this study, Table 2, imply that even at 723 K and 2 s holdup, the vapor phase conversion of tar would be <3.8% of tar. Thus reactor 1 tars reflect minimal contributions from secondary reactions and are taken as representative of the tars evolved near the wood surface. In the present work tars so evolved were defined as primary tars and the cumulative yields measured in mode 1 runs were used as the cumulative reactor 2 input yields for the kinetic modeling.

In mode 3 runs, reactor 2 was connected downstream of reactor 1, preheated, and then maintained isothermal. Homogeneous secondary reactions of wood tar vapors were studied quantitatively by measuring the effect of controlled thermal treatment of the tar in this reactor on product yields, tar loss, and tar molecular weight distributions. In practice this was accomplished by subjecting the tars to known combinations of reactor 2 temperatures (773–1,073 K) and tar residence times (0.9–2.2 s) to achieve a broad range of measurable tar conversions (<5–>88% of tar). Dispersion effects were neglected in the kinetic analyses presented below. Calculations using standard procedures (Levenspiel, 1972) yield a worst case reactor 2 vessel number of <0.01 (0.0091). Using this value in the small vessel number approximation of Wehner and Wilhelm's (1956) solution for effects of axial dispersion on first-order conversion (Levenspiel, 1972), one predicts that even at the highest reactor 2 temperature (1,073 K), the concentrations of tar exiting reactor 2 would exceed those for ideal plug flow under the same conditions by <18%. The nonidealities scale with the square of severity, and thus decline substantially with decreasing reactor 2 temperature. For example, this correction drops to <3% at 973 K. Since most of the present tar conversion data were obtained at temperatures of 973 or lower—Figure 2, below—neglect of axial dispersion is justified.

Products recovery and analysis

Total tar yield was determined from three separate measurements. The weight gains of the Teflon wool packed tubes and of the activated carbon packed traps were each measured gravimetrically. All tubing and valves in the reactor system were extracted by washing with pyridine to collect any tars condensed in the cooler sections of the system, such as the unheated connection upstream of the Teflon wool tar traps. The resulting solution was then dried in a warm water bath with nitrogen blowdown to inhibit volatiles loss, and the weight of the resulting residue was taken as the weight of extracted tar. Total tar yield

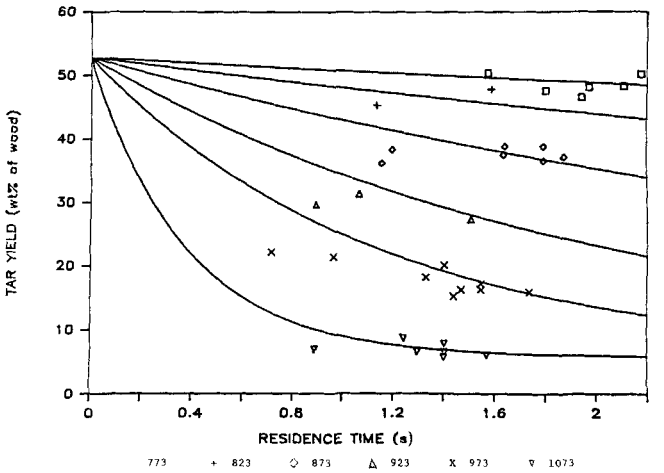

Figure 2. Single-reaction model correlation of tar yield as a function of temperature and residence time.

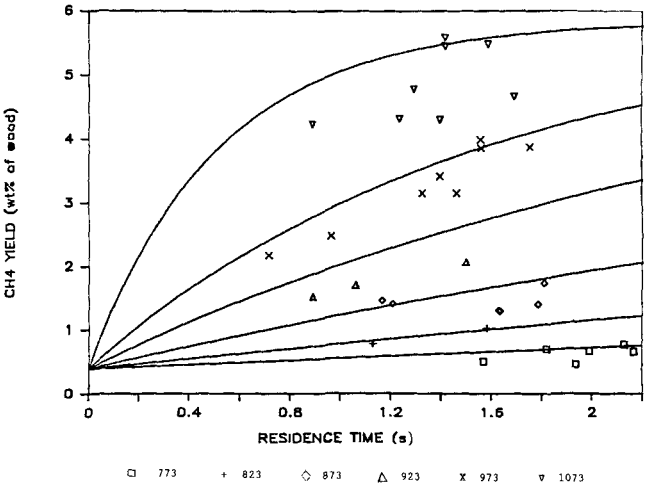

Figure 3. Single-reaction model correlation of methane yield as a function of temperature and residence time.

was the sum of these three tar measurements. Due to the small quantity of extracted tar (<1 wt. % of wood) compared to the tar in the traps, volatiles loss during drying of the extract is not important to the total tar yield measurement. Thus in this study tar is operationally defined as: organic volatile material from primary wood pyrolysis that is recovered from the tar traps and other system surfaces as described above. This definition differs from that of Nunn et al. (1985), who separately quantified some of the more volatile oxygenated liquids which, in the present study, are included as tar.

Product characterization has emphasized quantifying the yields of whole tar and light volatiles, and measurements of tar molecular weight distributions. A Perkin-Elmer Sigma 2B gas chromatograph was used to analyze the contents of each gas sampling loop for carbon monoxide, carbon dioxide, methane, acetylene, ethylene, ethane, and C_3 hydrocarbon gases. These assays together with the argon content of each sample and the overall carrier gas flow rate allowed the average rate of product evolution, at the time the gas sampling valve was filled, to be determined. Integration of these rates over the run time then allowed the cumulative yields of individual gases to be determined for a given temperature-time history in the volatiles generation reactor. Hydrogen yields were determined by analogous calculations using data on hydrogen evolution rates during the run, measured with a Fisher-Hamilton gas partitioner using an argon carrier.

Size-exclusion chromatography (SEC) was used to estimate the molecular weight distributions of the primary and secondary tars. The equipment is a Waters Associates ALC/GPC 201 SEC system with two μstyragel columns, 500 and 100 Å, in series, and a 405 nm UV detector. Pyridine was the SEC solvent. The SEC system was calibrated by vapor pressure osmometry (VPO) using actual wood pyrolysis tars. A tar sample was first separated into five different molecular weight fractions using a preparative scale SEC system. Each fraction was then analyzed by VPO and regular SEC to respectively determine their average molecular weight and molecular weight distribution. The two parameters for a linear calibration curve described by Yau et al. (1979), were then obtained by a best fit line for the five data points.

Mathematical modeling

Wood pyrolysis involves a complex set of parallel and series chemical reactions frequently influenced by heat and mass transfer. Fruitful approaches to modeling such a system can be based upon fairly drastic lumping of the reactant/products chemistry and other simplifying assumptions. The models used in this work assume the following reaction sequence:

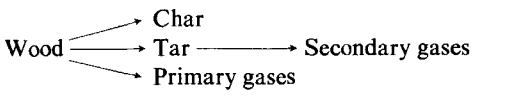

(1)

The models describe each of the above pathways with either a single-reaction or a distributed activation energy, first-order rate constant, the parameters for which are determined by curve-fitting product yield data. Nunn et al. (1985) have presented kinetic parameters for the formation of char, tar, and gases from rapid (~1,000 K/s) pyrolysis of thin samples of the same sweet gum hardwood used in this study. The present work focuses on systematic studies of the cracking of newly evolved vapors of wood pyrolysis tars, and on the resulting evolution of individual secondary gaseous products.

The first kinetic model used to correlate the data was the single first-order reaction model. This choice was reasonable, since this model has been used extensively with reasonable success for global correlations of the overall thermal conversion kinetics of other complex starting materials such as coal (Howard, 1981) and wood (Nunn, 1981; Nunn et al. 1985). Further, it is also probable that first-order bond scissions are important pathways in the dilute, vapor phase thermal decomposition of high molecular weight species, such as cracking of wood tar to lower molecular weight species. Net cumulative yields of unreacted tar and of individual gaseous products from tar vapor cracking were calculated as the difference between the cumulative amount of each entering (from mode 1 runs) and leaving (from mode 3 runs) reactor 2. The data were then fitted to the kinetic equation

$$\frac{dV_i}{dt} = k_i(V_i^* - V_i) \tag{2}$$

where V_i is the yield of material i at time t, V_i^* is the ultimate value of V_i at long residence times and high temperatures (determined as part of the fitting procedure by including experimental data at high conversions), and k_i is the global rate coefficient. Thus the rate of tar cracking at any time is modeled as first order in the difference between the ultimate (minimum) yield of tar (i.e., the "nonreactive" tar) and the total amount of tar unconverted at that time. This definition of ultimate yield for tar is a working definition based on the range of temperatures and residence times studied. At much higher reactor severities the ultimate tar yield is expected to be smaller or even zero. The rate of formation of an individual gaseous product is first order in the difference between the ultimate (maximum) yield of that gas and the amount of that gas generated up to that time. The kinetic parameters for homogeneous tar cracking and individual gaseous product formation were found by a least-squares parameter fitting technique.

The data were also correlated with a distributed activation energy model (DAEM) to increase the range of reaction conditions that could be fitted, compared to the single-reaction model. In this model the formation of each species is assumed to be the result of a large number of independent parallel first-order reactions with different rate constants. To simplify the mathematics, the rate constants for all reactions forming a single species are assumed to have an identical preexponential factor, A_{oi}. This simplification is reasonable since variations in the preexponential factor are expected to have less impact than activation energy on the rate behavior during monomolecular decomposition reactions of tar molecules. Thus all of the variation in kinetics is fitted by variations in the activation energy.

The activation energies are described by a continuous distribution function $f(E_i)$, where $f(E_i)dE_i$ represents the fraction of the total gas formed or tar cracked by reactions with activation energies between E and $E + dE$. Here, $f(E_i)$ is approximated by a Gaussian distribution with a mean activation energy of E_{oi} and a standard deviation of σ_i. Integration over the actual time-temperature history in reactor 2, including slight axial nonisothermalities, and over all possible activation energies then predicts

the yield of species i as a function of the kinetic parameters and the reaction conditions:

$$V_i = V_i^* \left[1 - \int_0^\infty \exp\left(- \int_0^t k_i \, dt \right) f(E_i) dE_i \right] \qquad (3)$$

The major advantage of the DAEM model over the single-reaction model is that the problem of low kinetic parameters that do not fit a large range of reaction conditions is eliminated (Howard, 1981). Low kinetic parameters in the single-reaction model are expected when forcing a single reaction to fit a temperature dependence that arises from the occurrence of different reactions in different temperature intervals. Instead, in the distributed activation energy model, a large number of reactions with a Gaussian distribution of activation energies occur independently in parallel.

By the addition of only a single parameter σ_i, a kinetic model is obtained that correlates a broader range of temperature and time conditions than the single-reaction model. Instead of the three parameters of the previous model (V_i^*, A_{oi}, E_i), this model uses four, replacing the activation energy with the mean and the standard deviation of the distribution of activation energies ($V_i^*, A_{oi}, E_{oi}, \sigma_i$). Although this model is more complex than the single-reaction model, especially under nonisothermal conditions commonly encountered in pyrolysis, the advantages of a better fit to the data and more reasonable kinetic parameters make this model more useful than the single-reaction analysis.

Results and Discussion

Approximately 100 runs were performed to generate a broad data base on product yields as a function of primary and secondary reactor operating parameters. Good material balances (95–102%), elemental balances (90–110%), and yield data reproducibility were obtained, and a broad range of tar conversions (<5–>88% of tar) was achieved in reactor 2.

Product yields

Representative yields for primary pyrolysis of wood and for different extents of homogeneous secondary tar cracking at 873, 973, and 1,073 K are shown in Table 1.

Comparison of mode 1 and mode 3 product yield data allowed identification of primary and homogeneous secondary products. Primary pyrolysis products were char, which remained in reactor 1, and the following volatiles which, in the tar cracking runs were conveyed to reactor 2: tar, water, carbon dioxide, carbon monoxide, and traces of methane.

Secondary reactants, and products arising from their secondary reactions, were identified by observing whether their yield increases, decreases, or remains constant when changing from a tar generation (mode 1) to a tar cracking (mode 3) run, or when increasing the mode 3 temperature. Tar, for example, is a primary product and a secondary reactant, as demonstrated by its high yield from mode 1 experiments and its decreasing yield with increasing reaction severity in mode 3 experiments. For residence times of about 1 s, homogeneous tar conversion was 30 wt. % at 873 K, and rose to 88 wt. % at 1,073 K.

Carbon dioxide appears to be both a primary and secondary product, since the yield in mode 1 is about half the total CO_2 yield from high-severity mode 3 runs (1,073 K, Table 1). Primary pyrolysis studies of Nunn et al. (1985) indicate that some CO_2 is formed at the earliest stages of primary wood pyrolysis when tar and water are also being formed. Those results indicate that at least some of the CO_2 observed in the present mode 1 runs is truly a primary product of wood pyrolysis. A fraction of the CO_2 obtained from mode 1 runs, however, could be the product of heterogeneous tar reactions to CO_2 within the packed bed of the generation reactor. Mode 3 runs, however, indicate that a large fraction (at least 50%) of the ultimate carbon dioxide yield is a secondary product of tar cracking rather than a primary product of wood pyrolysis. During homogeneous tar cracking, secondary yields of carbon dioxide can account for as much as 14% of the tar lost.

Table 1. Product Yields from Primary Pyrolysis and Different Extents of Homogeneous Secondary Tar Cracking

	Primary Yields wt. % wood	Yields After Different Extends of Tar Cracking, wt. % wood		
		873 K 1.2 s	973 K 1.0 s	1,073 K 1.0 s
Tar	52.8	36.6	16.6	6.1
Char	18.3	18.1*	18.4*	17.8*
CH_4	0.4	1.7	3.8	5.5
CO	3.2	14.7	25.7	35.7
CO_2	6.8	9.7	11.4	13.2
C_2H_2	0.0	0.1	0.5	0.6
C_2H_4	0.0	1.2	3.6	5.4
C_2H_6	0.0	0.1	0.3	0.4
H_2O	16.3	17.3	17.0	15.2
H_2	0.0	0.1	0.6	1.0
Total	97.8	99.6	97.9	100.9

*Remaining in reactor 1

Carbon monoxide and methane are evolved in modest quantities from reactor 1. However, most of the production of these compounds—along with acetylene, ethylene, ethane, and hydrogen—arises from secondary reactions, as evidenced by their substantial yield increases in the mode 3 experiments, Table 1.

Carbon monoxide was the major product of homogeneous secondary tar cracking at all temperatures, accounting for about 50–70 wt. % of the tar converted. Because CO yields are due almost solely to secondary tar cracking and because CO yields are very large, the yield of carbon monoxide could be used as an approximate indication of the extent of secondary cracking of dilute tar vapor in other wood pyrolysis systems. That CO and CO_2 account for over three-quarters of the tar that cracks at 1,073 K is not surprising given the high oxygen content (~40 wt. %) of the primary tar. Methane and ethylene respectively accounted for about 11 and 12 wt. % of the tar converted at 1,073 K. Most of the remaining few wt. % of the tar was cracked to form acetylene, ethane, and hydrogen, Table 1. At high tar cracking severities (>85%) the dry gas composition by volume was 48% CO, 19% H_2, 13% CH_4, 11% CO_2, and 7% C_2H_4, with traces of C_2H_2 and C_2H_6.

Negligible amounts of char were observed in reactor 2 upon completion of experiments on dilute homogeneous cracking of tar vapor. The ablative pyrolysis studies of Lede et al. (1983) found that char formation in wood devolatilization can be completely prevented by rapidly removing fresh pyrolysis tar liquids from wood surfaces at elevated temperature. This result indi-

cates that char is not a primary product of wood pyrolysis, but a secondary product from repolymerization of a low-volatility intermediate or tar. Together these two results indicate that char formation in wood pyrolysis involves tar reactions at higher concentrations than those studied here, or participation of condensed phases. Candidate pathways include liquid phase condensation reactions of tar (or tar precursors), and reactions of tar at higher vapor phase concentrations or at interfaces such as char.

Kinetics

Best fit kinetic parameters were obtained for homogeneous vapor phase cracking of newly formed tar and for formation of the resulting secondary product gases. The first model used to correlate the tar and gas data was the single first-order reaction model. The derived parameters are given in Table 2 along with the standard error of the estimate.

The extent of secondary reaction is a function of both temperature and time. The data for tar and methane yields are shown in Figures 2 and 3, respectively. Excellent correlation to the model is shown by the solid lines, except for tar yields at low residence times. The single reaction model consistently underpredicts the tar conversion at low residence times. Significant tar conversion (lower tar yields) would be expected even at short residence times if low activation energy reactions contribute to conversion, causing a more rapid decrease in the tar yield than one single, first-order reaction with a higher activation energy can fit. Further, the tar yields initially appear to decrease quite strongly, and then approach apparent temperature-dependent asymptotes, Figure 2. This behavior, and the underpredictions of short residence time conversions, are consistent with the occurrence of multiple independent parallel reactions, and support the use of the distributed activation energy model for a global description of these kinetics, see below.

Despite these limitations, overall the correlation of the present data with the single first-order reaction model was quite good. The results from this model also proved useful in comparing the present findings to previous literature. Vapor phase cracking of wood pyrolysis tars from an unspecified softwood was studied by Diebold (1985), and tar cracking during fluidized bed pyrolysis of poplar hardwood was studied by Liden (1985). Mattocks (1981) studied cracking of tars from both cherry and yellow pine. Due to major differences in the product group definitions as well as modeling techniques and assumptions, results from the present study could not be directly compared to the results of Mattocks.

The tar cracking rate constants of Diebold and Liden are

Table 2. Kinetic Parameters for Homogeneous Tar Cracking and Secondary Gas Formation, Single-Reaction Model

	log A s^{-1}	E kJ/mol	Y^* wt. % wood	SEE†
CH_4	4.89	94.2	5.83	0.12
C_2H_4	5.76	109	5.17	0.36
C_2H_6	7.52	139	0.38	0.03
CO_2	2.55	49.0	13.20	0.83
CO	4.66	87.9	36.33	1.8
H_2	6.64	129	1.09	0.08
Tar	4.98	99.3	5.79	2.2

Standard error of the estimate

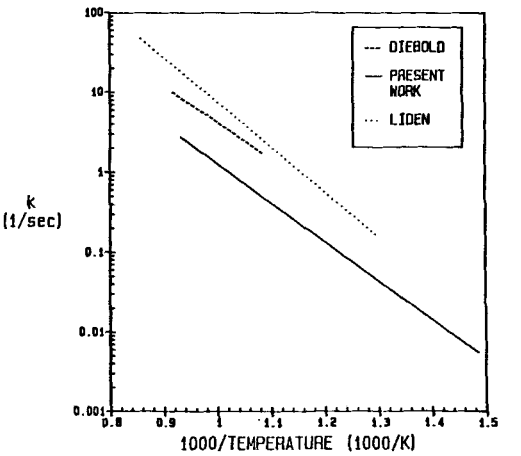

Figure 4. Comparison of single reaction tar cracking rate constant from three studies.

· · · Liden, 1985; --- Diebold, 1985; and —— present work

compared to the single-reaction model results of this study in Figure 4. Although Diebold modeled homogeneous tar cracking as a competitive reaction to form gases and a refractory residue, the yields of residue were so small that the reaction model was close to the simple single first-order reaction used in this study. For comparison, kinetic parameters for the cracking of volatiles to gases were:

	A, s^{-1}	E, kJ/mol
Diebold	$10^{5.19}$	87.5
Liden	$10^{6.49}$	108
This study	$10^{4.98}$	93.3

The results from this study are seen to be comparable to the results of both Diebold and Liden. Over the common temperature range of experimentation (923–1,073 K) the rate constant of Diebold is 3–3.5 times higher than that found in this work. Comparison with Liden's data over the common temperature range (773–1,073 K) indicates that the rate constant in his study is about six times higher than found in this study. These

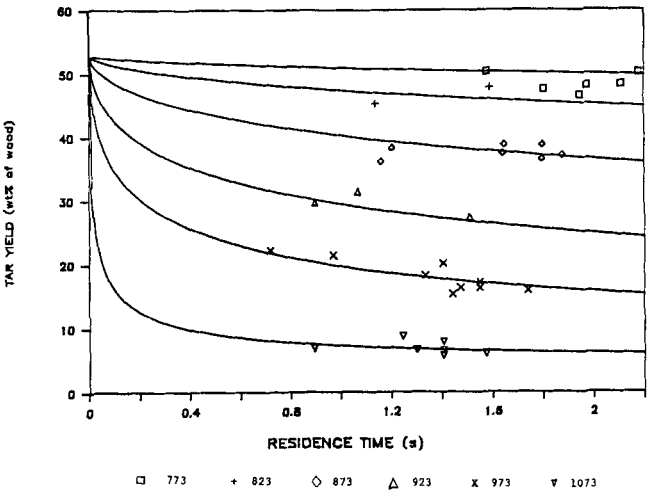

Figure 5. Distributed activation energy model correlation of tar yield as a function of temperature (K) and residence time.

discrepancies could be due to effects of wood type, reactor system, heating rates, or differences in the models.

Despite the approximate agreement with both Diebold's and Liden's tar cracking rates and the reasonable correlation of the data by the single first-order reaction model over most of the reaction conditions studied, this model is not completely satisfactory. Since the tar is a complex mixture of many organic compounds, its cracking and the attendant formation of individual secondary gases are not expected to proceed by single chemical reactions. Juntgen and Van Heek (1970) showed theoretically that a set of overlapping, independent, parallel first-order reactions can be approximated by a single first-order expression having both lower activation energy and lower preexponential factor than any of the reactions in the set (Howard, 1981). Thus, in the present analyses it is not surprising that forcing data representing a broad range of tar conversions to fit a single-reaction model results in a low activation energy and preexponential factor. One can think of the limitation as chemically reflecting the inability of one solitary reaction to adequately express a temperature dependence that, as severity range broadens, includes significant contributions from more and more reactions at higher and higher activation energies.

To avoid this limitation of the single-reaction model, the distributed activation energy model (DAEM) was used to correlate the tar and gas yields. The preexponential factor and activation energy were not independent parameters for these data; therefore, the preexponential factor was fixed at $10^{13}\ s^{-1}$, a reasonable value for gas phase decomposition reactions. The best fit parameters for tar cracking, individual gas formation, and total gas formation are given in Table 3. Here total gas (*Gas* in Table 3) is a separate lumped product category, equal to the total of the experimentally measured yields of CH_4, C_2H_4, C_2H_6, CO, CO_2, and H_2. These experimental totals were separately fitted to obtain the indicated kinetic parameters. The relatively small values for σ (~8% of E_o) account for the good fits with a single reaction model. For comparison, Anthony et al. (1975) reported a σ of 19% of E_o for pyrolysis of Montana lignite.

For the DAEM, conversion is a complex function of temperature, time, heating and cooling rates, and extent of reaction. For example, as the extent of reaction increases, the average activation energy of the remaining reactions increases due to the complete reaction of the low activation energy reactions. For the sake of comparison, however, the tar yield vs. equivalent isothermal time data of Figure 2 were approximated by the DAEM, assuming isothermal tar cracking, Figure 5. The calculation of equivalent isothermal time is based on the single-reaction parameters and is not exact for a distribution of activation energies. However, because the temperature profile is isothermal over 90% of the total time, the equivalent isothermal time is not significantly affected by the range of activation energies. For reactor 2 the ratio of the nonisothermal residence time t_n, to the total (nonisothermal + isothermal) residence time t_r scales approximately as $t_n/t_r = 0.1RT_f/E$, where T_f is the final reaction temperature, and E is the activation energy. Using the low value of E for tar cracking—that is, that for the single-reaction model, Table 2—and the highest cracking temperature (1,073 K), this relation gives a maximum nonisothermal contribution to t_r of <1%.

As shown by Figure 5, the distributed activation energy model is significantly better than the single-reaction model, Figure 2, at correlating the tar conversion data over the full range of reaction conditions. In particular, one notes the better ability of the DAEM to predict the rapid initial decrease in tar yields, apparently reflecting the inherent inclusion of low activation energy reactions in this model. In addition, the apparent asymptotic behavior of tar conversion with increasing residence time at a fixed temperature observed in this work, and reported by Antal (1983) for volatiles from pyrolysis of cellulose and lignin in steam, is also predicted by the distributed activation energy model.

Figure 5 also suggests another reason for the differences in the single-reaction kinetics of Diebold, Liden, and this study. In the present work, the single-reaction model fitted the data at residence times between 1.2 and 2.2 s, while Diebold fitted residence times of about 0.2 s and Liden times of 0.4–0.6 s. According to the DAEM, the data of this study and Liden appear to have been collected over the range of residence times where conversion is not a strong function of residence time. Apparent single-reaction rate constants for these runs would be inversely proportional to the residence time. The single-reaction rate constants for tar cracking from these runs, therefore, would be expected to differ by the ratio of residence times studied. Based on residence times, Liden's rate constants would be expected to

Table 3. Kinetic Parameters for Homogeneous Tar Cracking and Secondary Gas Formation DAEM

	$\log_{10} A$† s^{-1}	E kJ/mol	σ kJ/mol	V* wt. % wood	SEE‡
CH_4	13.0	242	23	6.10	0.10
C_2H_4	13.0	240	19	5.37	0.34
C_2H_6	13.0	236	11	0.37	0.03
CO_2	13.0	222	40	13.20	0.75
CO	13.0	236	23	37.91	1.2
H_2	13.0	249	17	1.16	0.08
Gas**	13.0	237	25	65.49	1.7
Tar	13.0	234	21	4.77	1.6

†Fixed
‡Standard error of the estimate
**Obtained by fitting combined experimental yields of CH_4, C_2H_4, C_2H_6, CO, CO_2, and H_2

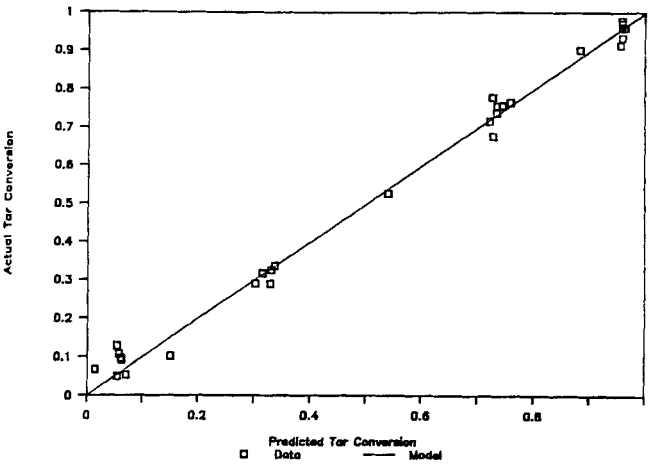

Figure 6. Actual vs. DAEM-predicted tar conversion during secondary thermal cracking.
Prediction from Table 3 parameters and experimental temperature-time histories
Units on axes are fractions of ultimate observed conversion

be three to five times larger than those from this study, which is not far from the reported ratio of about six times.

In Diebold's study the ratio of residence times would suggest that Diebold's rate constants would be six to ten times higher than those from this study, if conversions were near the apparent asymptotes. That Diebold's rate constants are only three to three and a half times higher than those of this study indicates that residence times of 0.2 s are short enough to observe the effect of residence time on conversion. This result is in agreement with the DAEM, as shown in Figure 5.

Conversions predicted with the DAEM are a complex function of the time-temperature history; however, from the actual time-temperature history and the best fit kinetic parameters the predicted tar conversion and yield of each secondary product can be calculated for each run. Plots of the actual experimental conversions of tar, and experimental yields of carbon monoxide and methane, vs. the corresponding predicted conversions or yields are shown in Figures 6–8, respectively. As shown, the correlation between the actual and predicted conversions and yields is good. As indicated by the decrease in the standard error of the estimate, Tables 2 and 3, the correlation of the data is better using the DAEM than with the single-reaction model, even though each model utilized three adjustable parameters. The distributed activation energy model also more closely fits the tar conversion data over a broader range of reaction temperatures and residence times than does the single-reaction model: compare Figure 5 with Figure 2.

Tar characterization

The tar samples collected after different extents of secondary thermal treatment were characterized by size-exclusion chromatography (SEC). Molecular weight distributions, from SEC, for a primary tar and for three tars surviving 9, 31, and 84% secondary conversion are shown in Figure 9. The area under each curve corresponds to the relative amount of tar recovered. A definite shift toward lower molecular weight tars with increasing reaction severity is seen. This shift is expected in cracking reactions; however, the distributions also show no shift toward molecular weights greater than those of the primary

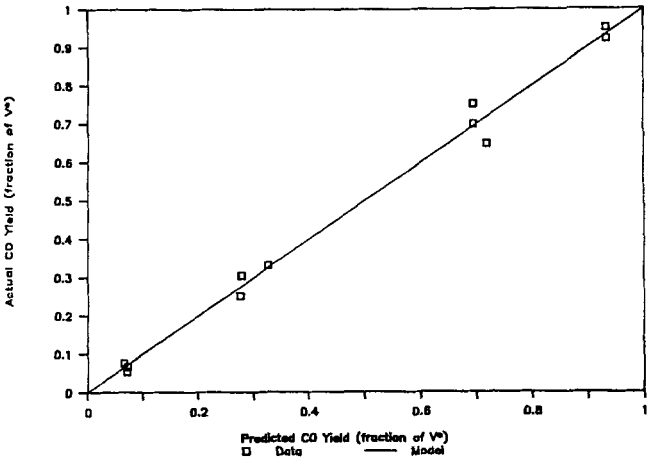

Figure 7. Actual vs. DAEM-predicted CO yield during secondary thermal cracking.
Prediction from Table 3 parameters and experimental temperature-time histories

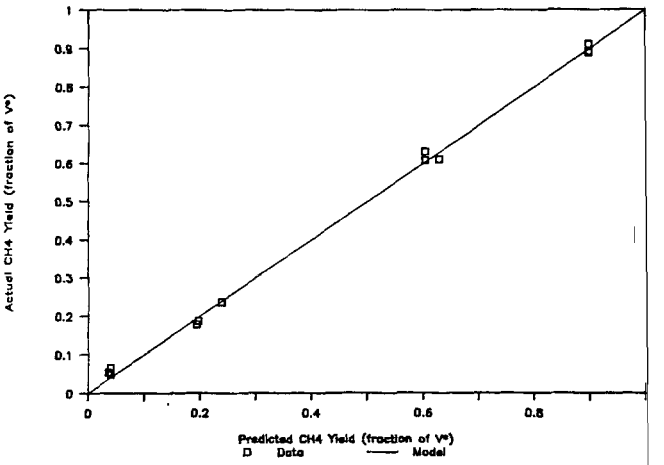

Figure 8. Actual vs. DAEM-predicted CH_4 yield during secondary thermal cracking.
Prediction from Table 3 parameters and experimental temperature-time histories

tars. The latter result indicates that little or no repolymerization of the tar is brought about by dilute vapor phase cracking.

The weight-average molecular weight of the tars as affected by conversion is presented in Figure 10. As shown, the average molecular weight of tar surviving secondary cracking is lower than the molecular weight of primary tar (640 g/gmol) entering the cracking reactor. Average molecular weights tend to decrease with increasing conversion, Figure 10; however, the change in average molecular weight over the range of conversion, 10–80%, is small after a sharp drop in average molecular weight from 0 to 10% conversion.

Conclusions

The experimental results of this study identified and quantified major products generated by primary pyrolysis of small packed beds (~2 cm deep) of wood at 0.2 K/s, and by vapor phase secondary cracking of the resulting newly formed wood pyrolysis tar, at low molar concentrations, temperatures from 773–1,073 K, and residence times of 0.9–2.2 s. Tar, char, water, and carbon dioxide are primary pyrolysis products, with tar

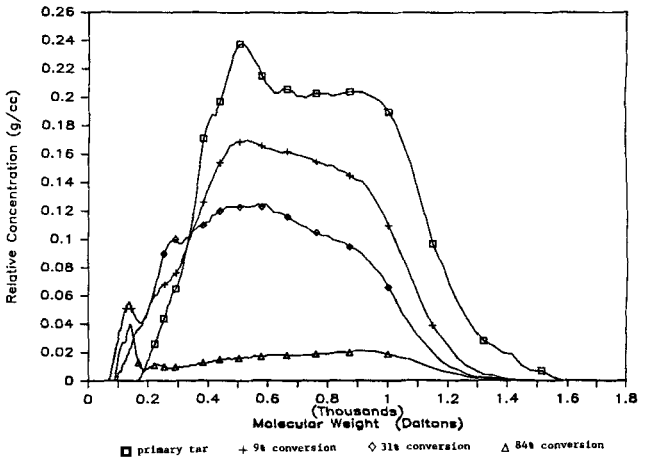

Figure 9. Molecular weight distributions for primary pyrolysis tar and three tars surviving different extents of homogeneous thermal cracking.

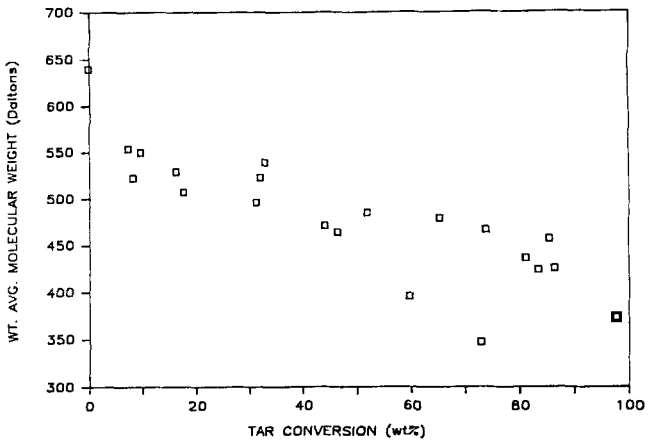

Figure 10. Weight-average molecular weight of tar as a function of homogeneous conversion.

yields exceeding 50 wt. % of the parent wood. Modest amounts of CO and trace quantities of methane are also observed from primary pyrolysis of the wood. Additional carbon dioxide is formed by vapor phase cracking of tar. The major tar conversion product was carbon monoxide, which accounted for over two-thirds of the tar lost at high severities. Corresponding ethylene and methane yields were each about 10% of the converted tar. Coke formation was negligible in the cracking reactor. Size-exclusion chromatography indicated that tars surviving vapor phase cracking are lower in weight-average molecular weight than the uncracked tars, and there is no shift in tar molecular weight to values higher than the molecular weight of primary tar. The latter finding suggests that there is little or no repolymerization of tar during dilute vapor phase cracking.

A first-order single-reaction model generally correlated the experimental yields of the individual gaseous products of the tar cracking to within better than 10%, but seriously underpredicted low residence time tar conversions. The single-reaction kinetic parameters for tar cracking from this work approximately agreed with single-reaction rate parameters obtained by both Diebold (1985) and Liden (1985) for cracking of wood volatiles. A distributed activation energy model outperformed the present single-reaction model by better correlating the tar conversion behavior over a broader range of residence times and temperatures. The DAEM model also fitted temperature-dependent apparent asymptotes observed in data on tar conversion as a function of residence time.

Acknowledgment

Most of the above work was supported by the National Science Foundation, Division of Chemical and Process Engineering, Materials Engineering Program, under Grant Nos. CPE-8212308 and CBT-8503664. We also gratefully acknowledge an NSF Fellowship for M. L. Boroson and financial support by the Edith C. Blum Foundation of New York, NY, and the Robert C. Wheeler Foundation of Palo Alto, CA. Undergraduate researchers Christine Clement and Anne Reeves have made valuable contributions to this work. Samples of sweet gum hardwood, milled wood lignin, and other wood constituents were specially prepared for our biomass research program by H-M. Chang and his colleagues in the Department of Wood and Paper Science at North Carolina State University, who are gratefully acknowledged.

Notation

A_{oi} = Arrhenius preexponential factor for species i, s^{-1}
E_i = apparent Arrhenius activation energy for species i, kJ/mol
E_o = mean of Gaussian activation energy distribution function, kJ/mol
$f(E)$ = distribution function for activation energies
$k_i = A_i \exp(-E_i/RT)$ = Arrhenius rate constant, s^{-1}
V_i = yield of species i, wt. % wood
V_i^* = ultimate yield of species i, wt. % wood
σ = standard deviation of activation energy distribution, kJ/mol

Literature Cited

Antal, M. J., Jr., "Effects of Reactor Severity on the Gas-Phase Pyrolysis of Cellulose and Kraft Lignin-Derived Volatile Matter," *Ind. Eng. Chem. Prod. Res. Dev.*, **22**, 366, (1983).

Anthony, D. B., J. B. Howard, H. C. Hottel, and H. P. Meissner, "Rapid Devolatilization of Pulverized Coal," *Proc. 15th Int. Symp. on Combustion*, Combustion Inst., Pittsburgh, 1303 (1975).

Boroson, M. L., "Secondary Reactions of Tars from Pyrolysis of Sweet Gum Hardwood," Ph.D. Thesis, Dept. Chem. Eng., MIT, Cambridge, MA (1987).

Chan, R., and B. B. Krieger, "Modeling of Physical and Chemical Processes During Pyrolysis of a Large Biomass Pellet with Experimental Verification," *Am. Chem. Soc. Div. Fuel Chem. Prepr.*, **28**(5), 330, (1983).

Diebold, J. P., "The Cracking Kinetics of Depolymerized Biomass Vapors in a Continuous, Tubular Reactor," M.S. Thesis, Dept. Chem. Petroleum-Refining Eng., Colorado Sch. Mines, Golden (1985).

Howard, J. B., "Fundamentals of Coal Pyrolysis and Hydropyrolysis," *Chemistry of Coal Utilization, 2d suppl. vol.*, M. A. Elliott, ed., Wiley, New York, ch. 12 (1981).

Juntgen, H., and K. H. Van Heek, "Reacktionablaufe unter nichtisothermen Bedingungen," *Fortschritte der chemischen Forschung*, **13**, Springer, Berlin, 601 (1970); trans., Belov and Assoc., Denver, CO, APTIC-TR-0776.

Kelbon, M., S. Bousman, and B. Krieger-Brockett, "Conditions that Favor Tar Production from Pyrolysis of Large, Moist Wood Particles," *Am. Chem. Soc. Div. Fuel Chem. Prepr.*, **32**(2), 44 (1987).

Lede, J., J. Panagopoulos, and J. Villermaux, "Experimental Measurement of Ablation Rate of Wood Pieces Undergoing Fast Pyrolysis by Contact with a Heated Wall," *Am. Chem. Soc. Div. Fuel Chem. Prepr.*, **28**(5), 383 (1983).

Levenspiel, O., *Chemical Reaction Engineering*, 2d ed., Wiley, New York, 282 (1972).

Liden, A. G., "A Kinetic and Heat Transfer Modelling Study of Wood Pyrolysis in a Fluidized Bed," M.A.Sc. Thesis, Dept. Chem. Eng., Univ. Waterloo, Ontario, Can. (1985).

Mattocks, T. W., "Solid and Gas Phase Phenomena in the Pyrolytic Gasification of Wood," M.S. Thesis, Dept. Mech. Aerospace Eng., Princeton Univ., New Jersey (1981).

Nunn, T. R., "Rapid Pyrolysis of Sweet Gum Wood and Milled Wood Lignin," M.S. Thesis, Dept. Chem. Eng., MIT, Cambridge, MA (1981).

Nunn, T. R., J. B. Howard, J. P. Longwell, and W. A. Peters, "Product Compositions and Kinetics in the Rapid Pyrolysis of Sweet Gum Hardwood," *Ind. Eng. Chem. Process Des. Dev.*, **24**, 836 (1985).

Serio, M. A., "Secondary Reactions of Tar in Coal Pyrolysis," Ph.D. Thesis, Dept. Chem. Eng., MIT, Cambridge, MA (1984).

Serio, M. A., W. A. Peters, and J. B. Howard, "Kinetics of Vapor-Phase Secondary Reactions of Prompt Coal Pyrolysis Tars," *Ind. Eng. Chem. Res.*, **26**, 1831 (1987).

Wehner, J. F., and R. H. Wilhelm, "Boundary Conditions of Flow Reactor," *Chem. Eng. Sci.*, **6**, 89 (1956).

Yau, W. W., J. J. Kirkland, and D. P. Bly, *Modern Size-Exclusion Liquid Chromatography*, Wiley-Interscience, New York (1979).

Manuscript received July 22, 1987, and revision received July 18, 1988.